ISSN 0965-545X, Polymer Science, Series A, 2016, Vol. 58, No. 4, pp. 567–577. © Pleiades Publishing, Ltd., 2016.

COMPOSITES

The Physical and Mechanical Properties and Cure Characteristics of NBR/Silica/MWCNT Hybrid Composites[1]

M. M. Salehi*, T. Khalkhali, and A. A. Davoodi

Polymer and Science Technology Division, Research Institute of Petroleum Industry, Tehran, 1599653111 Iran

**e-mail: salehimm@ripi.ir*

Received July 13, 2015; Revised Manuscript Received December 23, 2015

Abstract—The main objective of the present study was to investigate the synergistic effect of simultaneous use of two reinforcing fillers in rubber compounds based on acrylonitrile-butadiene copolymer (NBR). Silica was used as reinforcing filler in all samples and the loading content was 25 phr. 3 and 5 phr of multiwall carbon nanotubes (MWCNT) were used as second reinforcing filler in NBR/silica compounds. Melt mixing method was employed for compound preparation. The effects of carbon nanotube/silica hybrid filler on mechanical and vulcanization characteristics of the rubber compounds were investigated. These results revealed that addition of the reinforcing filler, either carbon nanotube or silica, shortened the optimum cure time (t_{90}) and also scorch time (t_{s1}) of samples compared to that of pure NBR compound. In hybrid compounds, the reduction in optimum cure time and scorch time was higher than that of for silica-filled NBR or CNT-filled NBR compounds. This can be attributed to the synergistic effect between CNT and silica as two reinforcing agents in NBR compounds. Regardless the composition of the reinforcing filler, an increase of the relaxed storage modulus is observed, while the tan δ value is decreased steadily. The dynamic modulus reinforcement of nanocomposites was examined by the Guth Gold and Modified Guth Gold equations. For hybrid samples, the experimental values show a significant positive deviation from model predictions. According to the Barlow's formula, hybrid compounds show higher burst strength compared to silica or CNT filled NBR compounds.

DOI: 10.1134/S0965545X16040131

INTRODUCTION

Acrylonitrile-butadiene copolymer (NBR) is a special purpose elastomer that possesses attractive properties, such as good oil resistance, abrasion resistance, elastic properties and low gas permeability, and is widely applied in a wide range of industrial equipment [1]. However, the mechanical properties, ozone resistance and processability of NBR are poor [2]. Fillers such as silica, carbon black, layered silicates, and carbon nanotubes are usually added to improve its physical properties and mechanical strength [3–12].

The extent of property improvement depends on several factors including the size of the particles, their aspect ratio, their degree of dispersion and orientation in the matrix and the strength of interactions between the filler and the matrix polymer [3]. However, the addition of fillers has some limitations and desired properties cannot be achieved. The idea of combination of fillers in order to make use of synergistic effects which can be used as a convenient method to improve the properties of elastomeric compounds is discussed [1, 3–5, 8, 11, 13]. In this regards, a combination of silica (SiO_2) and carbon black (CB) in different matrix systems have been widely studied and concluded that the mixture of silica and CB has highly efficient to lower the rolling loss and to improve the wet skid resistance so as to produce green tires with limited energy consumption and CO_2 emission from automobiles. Bendahou et al. [13] investigated the synergistic effect of nanoclay and cellulose whiskers on the mechanical and barrier properties of natural rubber (NR) composites. They found that the nanoclay dispersion state was totally modified as cellulose whiskers were introduced in the matrix. The calculated tortuosity values indicated that the simultaneous use of nanoclay and whiskers could greatly slow down the gas diffusion rate in NR. Formation of nanoclay-whiskers subassembly should be responsible for this synergistic effect. Chen et al. [1] investigated the thermal degradation behavior of hydrogenated nitrile-butadiene rubber (HNBR) with clay and carbon nanotubes (CNT). They show that the HNBR/clay/CNTs nanocomposites had lower thermal degradation rate than HNBR/clay, which could be attributed to that the clay-CNTs filler network reduced the diffusion speed of degradation products. The coexistence of clay and CNTs could form compact char layers with better barrier properties and thus improve the thermal stability of HNBR.

[1]The article is published in the original.

Table 1. Formulation of NBR compounds

Ingredients*	NBR0:0	NBR25:0	NBR0:3	NBR0:5	NBR25:3	NBR25:5
NBR	100	100	100	100	100	100
Silica	0	25	0	0	25	25
CNTs	0	0	3	5	3	5
DOP	15	15	15	15	15	15
IPPD	1.5	1.5	1.5	1.5	1.5	1.5
ZnO	5	5	5	5	5	5
ST.A.	1	1	1	1	1	1
TMTD	1.5	1.5	1.5	1.5	1.5	1.5
CBS	1.5	1.5	1.5	1.5	1.5	1.5
Sulphur	1.5	1.5	1.5	1.5	1.5	1.5

* Amount indicated here is in parts per hundred gram rubber (phr) basis.

Praveen et al. [4] evaluated the structure-properties of SBR/nanoclay/carbon black (CB) hybrid nanocomposites. Tensile results of CB filled SBR nanocomposites show remarkable improvement in strength properties. This suggests a synergistic between CB and nanoclay.

Except carbon black, silica is one of the most important filler used in the NBR compound. Nitrile rubber exhibited the highest interaction with silica probably through the hydrogen bond between the –CN group and silanol groups. In addition, silica (SiO_2) as reinforcing filler has been preferentially selected for preparing vulcanizates with a unique combination of tear strength, abrasion resistance, age resistance, and adhesion properties.

To our best knowledge, there is no report on the use of combination of silica with other fillers such as carbon nanotubes for improving the physical and mechanical properties of NBR compounds. In this regards, we investigated the synergistic effect of silica with carbon nanotubes on the physical, mechanical and curing properties of NBR compounds.

EXPERIMENTAL

Materials

The basic materials used in this work were: NBR with 45 wt% acrylonitrile (ACN) (Mooney viscosity (ML 1 + 4, at 100°C) = 60) was provided by Polimeri Europa Co., Ltd. The precipitated silica (VN3) powder with a surface area 175 m^2/g comes from Evonik Degussa, Germany. Multi-wall carbon nanotubes (CNTs) with 10–20 nm outer diameters were made in Cheap Tube Co., Ltd. Other compounding (DOP oil) and curing additives (ZnO, Stearic acid, Sulphur, CBS, TMTD), including antioxidant (IPPD-4010) are commercial grades.

Sample Preparation

All samples were prepared by melt compounding on a two-roll mill with a friction ratio of 1.0 : 1.4 at 50°C. Vulcanization characteristics of the samples were determined by Monsanto Oscillating Disk Rheometer 100 at 150°C. After mixing, the rubber compounds were left for 12 h and then molded in the form of sheets in an electrically heated hydraulic press at their optimum cures obtained from rheometer at 150°C. The denoted codes and composition of the samples are described in Table 1.

Sample Characterization

Cure properties of the rubber compounds. The scorch time (t_{s1}), which is the time for the onset of cure, and the optimum cure time (t_{90}), which is the time for the completion of cure, were determined by Monsanto Oscillating Disk Rheometer 100 at 150°C. ΔM, which is the difference between the maximum and minimum torque values on the cure trace of the rubber. The cure rate index (CRI), which is a measure of the rate of curing in the rubber, was calculated using,

$$\mathrm{CRI} = 100/(t_{90} - t_{s1}) \quad (1)$$

Scanning electron microscopy (SEM). The filler dispersion state was observed at different scales using scanning electron microscope, SEM, (Hitachi 4160, Japan) with 20 kV accelerating voltage. The cryogeni-

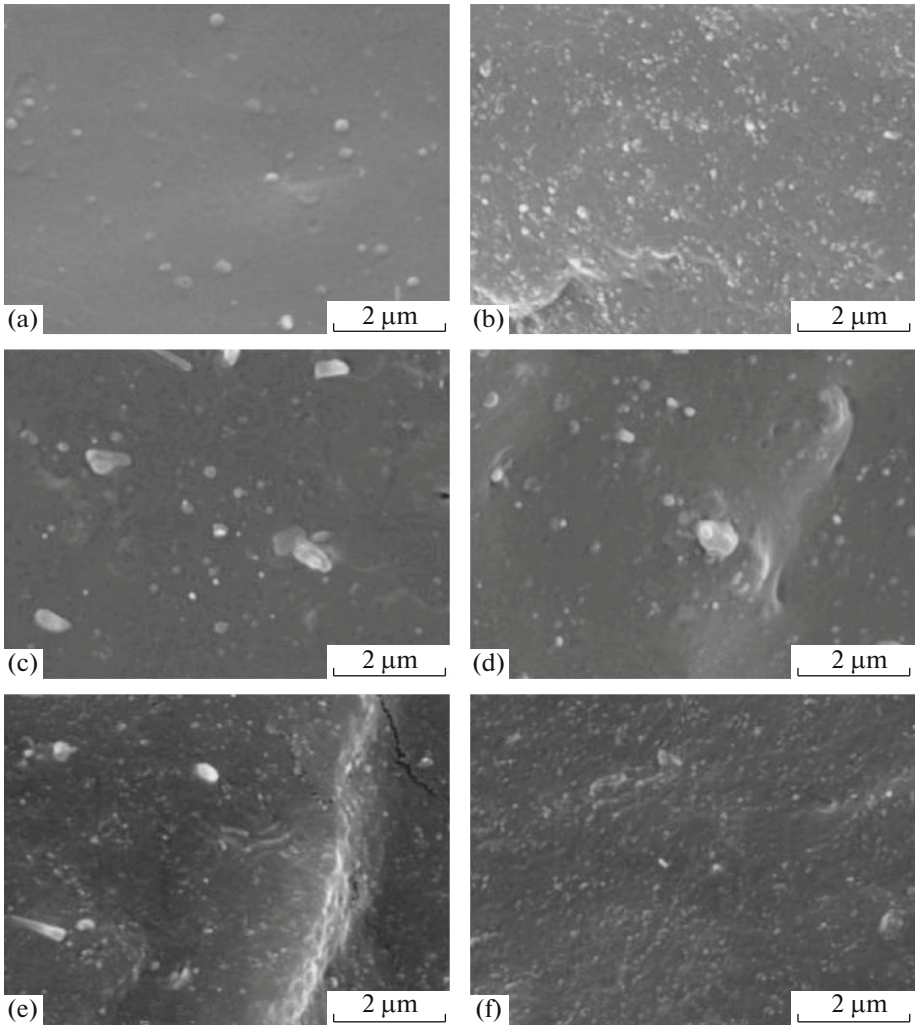

Fig. 1. SEM observation of NBR compounds at 15000 magnification: (a) NBR0:0, (b) NBR25:0, (c) NBR0:3, (d) NBR0:5, (e) NBR25:3, and (f) NBR25:5.

cally fractured surfaces were coated with gold for enhanced conductivity using SPI sputter coater.

Mechanical properties. Tensile specimens were punched out from the molded sheets using ASTM Die-C. The tests were carried out as per the ASTM D 412 methods in a Gotech Testing Machines Inc. (Gotech/GT-7016-A, Taiwan) at a cross head speed of 500 mm/min. Results were averaged on five measurements. IRHD hardness was measured with a Zwick hardness tester according to the standard ASTM D2240.

Dynamic mechanical thermal analysis (DMTA). The dynamic mechanical thermal analysis was conducted using rectangular samples having dimensions of 25 × 10 × 2 mm on DMTA machine, Triton-Tritec 2000, United Kingdom. The dynamic temperature sweep tests were conducted at 1 Hz frequency and 0.05% strain within temperature ranges of −100 to +100°C.

RESULTS AND DISCUSSION

Morphological Study

It is well known that the dispersion of fillers in polymer matrix is a key factor for the reinforcement of mechanical properties of polymer composites. In this work, the dispersion of silica and CNT in NBR matrix and their interaction in presence of NBR can be obtained by the SEM micrographs as shown in Figs. 1 and 2.

In pure NBR sample (NBR0:0), there is no agglomerate or aggregate, so the SEM micrograph is clear. However, in the NBR25:0, NBR25:3 and NBR25:5 samples, silica aggregates are visible as small white spots on the background. In NBR0:3 and NBR0:5 samples the CNT are visible and it can be seen with the 60000x magnification (Fig. 2). As it can be seen all samples show good dispersion and distribution of silica and CNT. It may be due to the good affinity between the reinforcing fillers with NBR

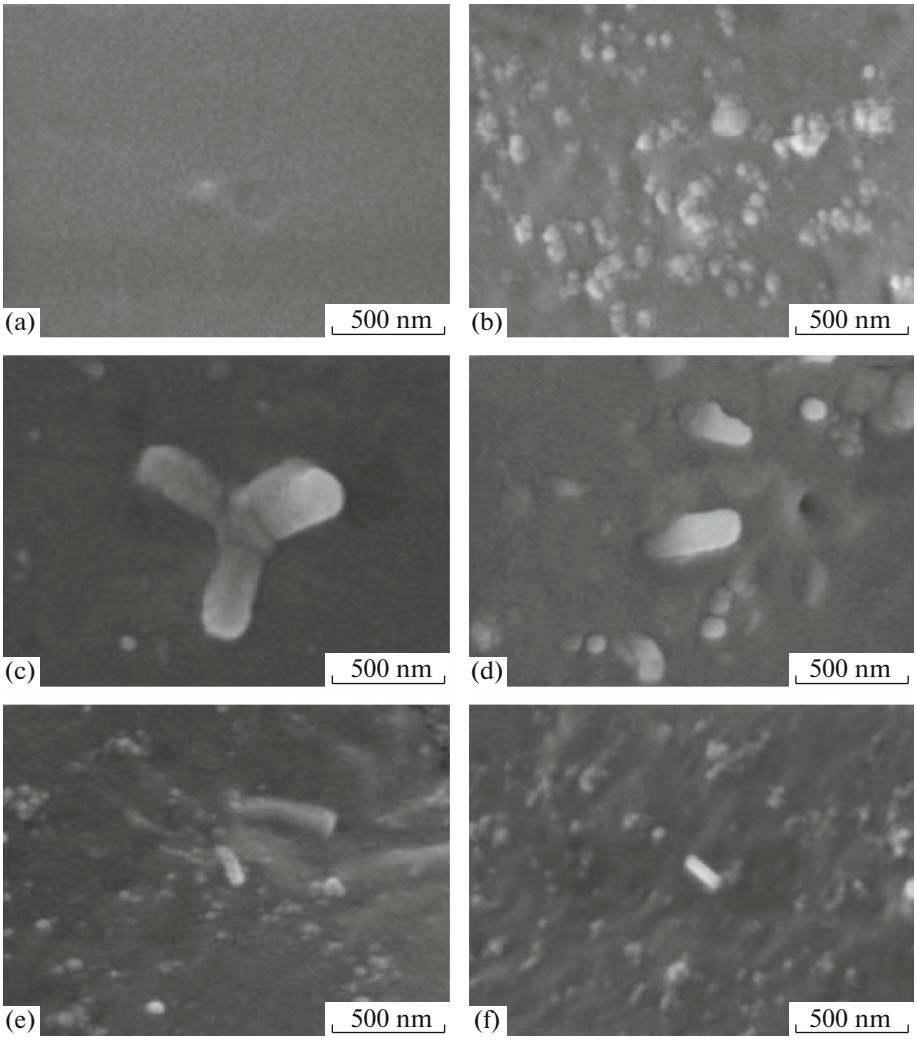

Fig. 2. SEM observation of NBR compounds at 60000 magnification: (a) NBR0:0, (b) NBR25:0, (c) NBR0:3, (d) NBR0:5, (e) NBR25:3, and (f) NBR25:5.

matrix. NBR has polar nitrile groups (–CN). Particles surfaces of silica have hydrophilic silanol groups (–Si–OH). Because the silanol group of silica is acidic and the nitrile group of NBR is basic, they can make a good hydrogen bond [15, 22]. However, in CNT filled samples (NBR0:3, NBR0:5, NBR25:3 and NBR25:5) more holes formation and detachment of the fillers on the surface of composites. This implies the weaker interaction between CNT and NBR matrix compared to that of silica and NBR matrix.

Curing Characteristics

Vulcanization graphs of the NBR compounds were shown in Fig. 3. Corresponding data obtained from the vulcanization analysis including optimum cure times (t_{90}, t_{s1}), cure rate index and torque values ($\Delta M = M_H - M_L$) are given in Table 2.

Comparing to the results revealed that addition of the reinforcing filler, either carbon nanotube or silica, shortened the optimum cure time (t_{90}) and also scorch time (t_{s1}) of samples compared to that of pure NBR compound (NBR0:0). On the other hand, the optimum cure time and scorch time both decrease with adding the silica to NBR compounds. This phenomenon can be explained by different mechanisms. In the first mechanism, the reduction was associated with the increase in the compound viscosity and thus the shear heating effect. In the second mechanism, the reduction in cure time can be explained by the increase in effective filler volume by bound rubber for the silica. In fact, NBR chains can be adsorbed on the silica surface, which reduces the volume available for chemicals and thus increases the concentration of the curing agents in the free polymer. This will result in faster onset and higher rate of vulcanization with respect to the neat rubber with no filler. This phenom-

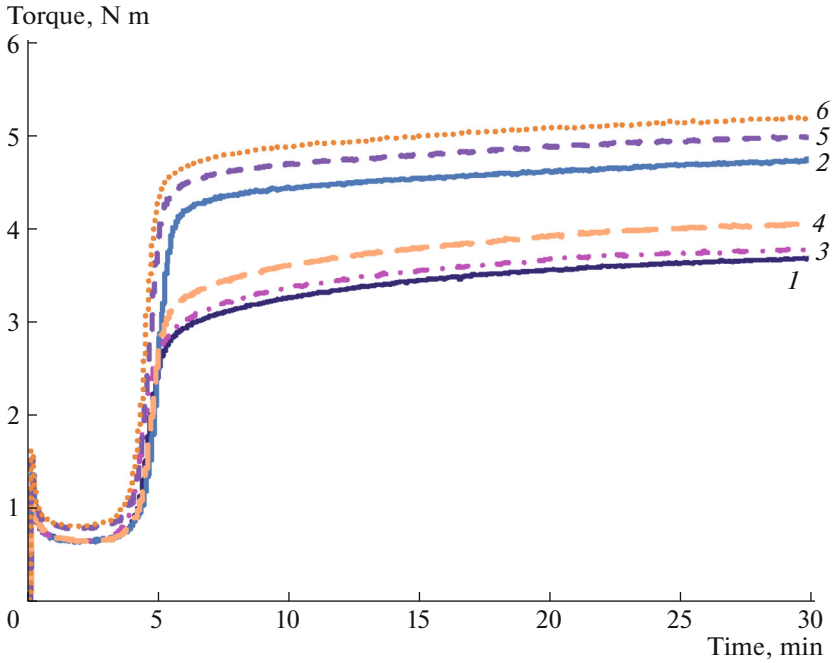

Fig. 3. (Color online) Cure curves of the NBR compounds at 150°C: (*1*) NBR0:0, (*2*) NBR25:0, (*3*) NBR0:3, (*4*) NBR0:5, (*5*) NBR25:3, and (*6*) NBR25:5.

enon can be correlated to the strength of filler-polymer interaction rather than the chemistry of filler surface which was explained by Wang et al. [17].

For the carbon nanotube compound, a reduction in cure time and scorch time compared to the pure NBR compound can be seen. The presence of the CNT seems to speed curing up. Scorch time was affected by the CNT. In these cases there was a small decrease in scorch time compared to the pure NBR and compounds containing silica. This reduction in cure and scorch time in CNT-filled NBR compounds for reasons similar to those given for the effect of the silica loading, as stated earlier.

In hybrid compounds (NBR25:3 and NBR25:5) the reduction in optimum cure time and scorch time was higher than that of for silica-filled NBR or CNT-filled NBR compounds. This can be attributed to the synergistic effect between CNT and silica as two reinforcing agents in NBR compounds.

Table 2 also compares the torque differences ($\Delta M = M_H - M_L$) measured for the elastomer compound samples. The rising trend of torque differences with addition of filler to the NBR compound could be ascribed to the compound viscosity corresponding to the interactions established between the rubber matrix and the reinforcement. The results show that, increasing the torque differences for NBR25:0, NBR25:3 and NBR25:5 compounds were higher than that of for NBR0:3 and NBR0:5 compounds. In fact, the strong interactions between NBR functionalities and the silanol groups present at the silica surface might be responsible for this behavior.

Table 2. Vulcanization characteristics of the NBR compounds at 150°C

	NBR0:0	NBR25:0	NBR0:3	NBR0:5	NBR25:3	NBR25:5
M_H, N m	3.7	4.7	3.7	4.0	5.0	5.1
M_L, N m	0.6	0.6	0.7	0.6	0.8	0.8
$M_H - M_L$, N m	3.1	4.0	3.1	3.4	4.2	4.3
t_{90}, min	14	6.8	12	11.4	6.2	6.3
t_{s1}, min	3.7	3.6	3.6	3.5	3.5	3.4
Cure rate index, min^{-1}	9.7	32.2	11.7	12.8	37.2	34.5

Table 3. Rubbery storage tensile modulus E' estimated at 25°C (E'_{25}), and temperature position (T_g) and magnitude (I_α) of the main relaxation process for NBR compounds

Sample	E'_{25}, MPa	T_g, °C	I_α
NBR0:0	1.6	−14	1.7
NBR25:0	7.3	−4	1.2
NBR0:3	2.3	−12	1. 6
NBR0:5	2.5	−11	1.5
NBR25:3	8.2	−1	1.1
NBR25:5	9.6	0	1.1

Mechanical Properties

Dynamic mechanical analysis (DMTA). The plots of storage modulus and tan δ vs. temperature of NBR and NBR compounds are shown in Figs. 4 and 5, respectively. The curve of log (E') corresponding to the pure NBR compound (NBR0:0) is typical of a fully amorphous thermoplastic polymer. For temperatures below the glass transition temperature, NBR is in the glassy state and its storage modulus slightly decreases with temperature but remains roughly constant. Then, a sharp decrease over three decades is observed around −14°C, corresponding to the main relaxation phenomenon, associated to the anelastic manifestation of the glass transition. It results in an associated well-defined maximum of the loss angle (Fig. 5). Then, the modulus reaches a plateau, corresponding to the rubbery state. At room temperature (25°C), the rubbery modulus was around 1.65 MPa (Table 3).

Regardless the composition of the reinforcing filler, an increase of the relaxed storage modulus is observed (Fig. 4), while the tanδ value is decreased steadily. The decreasing tanδ value can be attributed to the strong mutual interaction between NBR and silica and/or CNT that decreases the interfacial slide and relaxation. This phenomenon ultimately results in decreasing lag and thereby lowering of tan δ value. The interfacial interaction is strong because of good dispersion of the CNT tubes and/or silica particles in NBR, and the tubes and/or particles can function as pseudo-crosslinking points, which results in markedly increasing storage modulus of NBR composites containing silica and/or CNTs [5, 8–10].

After relaxation, the storage modulus observed particularly at the rubbery plateau regions are noted to be a decade higher for silica filled NBR sample (NBR25:0) than that of CNT filled NBR samples (NBR0:3 and NBR0:5), this may be attributed to the higher volume fraction of silica compared to CNT in NBR matrix.

However, for hybrid samples (NBR25:3 and NBR25:5) the strong increase of the storage modulus and decrease of the magnitude of the loss angle (tanδ) are most probably related to synergistic effect of the two filler in NBR matrix. The polymer chains can be adsorbed on the filler surface which reduces the seg-

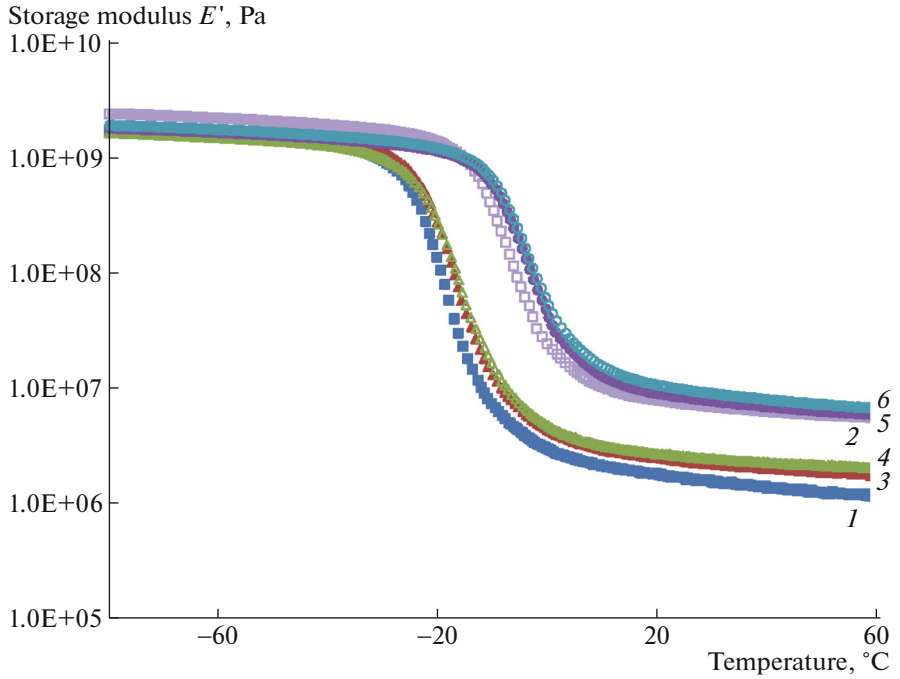

Fig. 4. (Color online) Storage modulus vs. temperature plot of NBR compounds: (*1*) NBR0:0, (*2*) NBR25:0, (*3*) NBR0:3, (*4*) NBR0:5, (*5*) NBR25:3, and (*6*) NBR25:5.

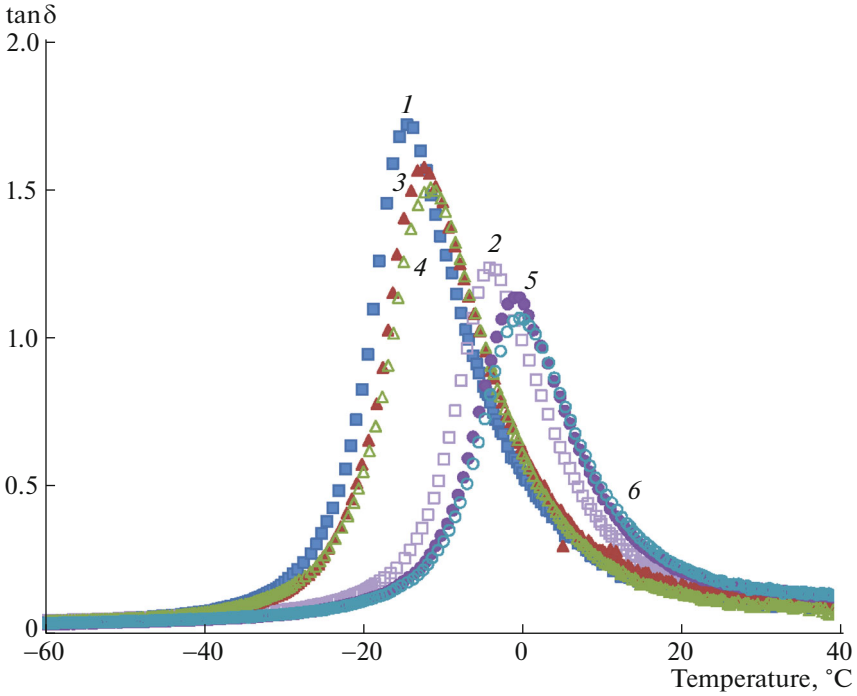

Fig. 5. (Color online) Loss angle (tanδ) vs. temperature plot of NBR compounds: (*1*) NBR0:0, (*2*) NBR25:0, (*3*) NBR0:3, (*4*) NBR0:5, (*5*) NBR25:3, and (*6*) NBR25:5.

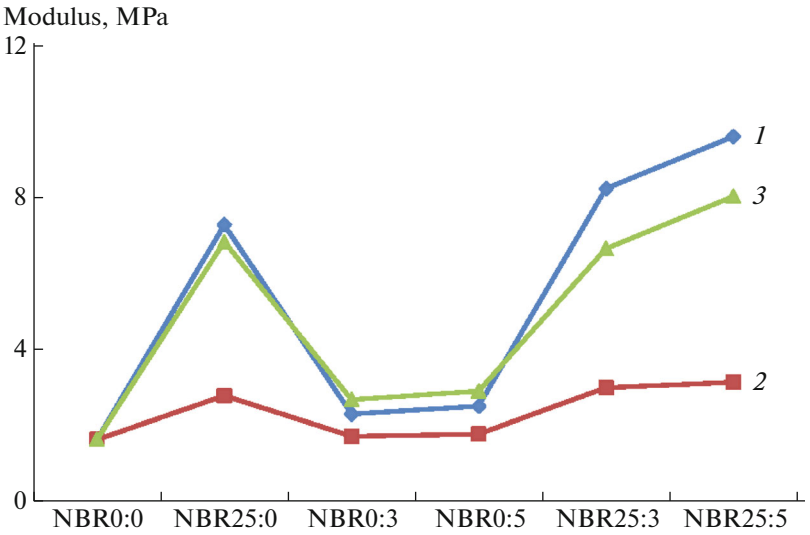

Fig. 6. (Color online) Comparison amongst experimental storage modulus and different models predicated modulus of NBR compounds. (*1*) *E*' Experimental, (*2*) Guth Gold Model, (*3*) Modified Guth Gold Model.

mental mobility of the polymer chains [18]. These results in formation of a rubber shell having the high modulus near the filler surface. As the polymer chains move a distance from the filler surface, the modulus value gradually decreases, and the value ultimately reaches the same level as that of the polymer matrix [16]. When two or more aggregates (silica particles and CNT tubes) are close enough, they form agglomerate via an adjoining rubber shell where the modulus of the occluded polymer is higher than that of the bulk polymer matrix. The immobilized polymer chains attached to the filler, can lead to an increase in effective volume fraction of the filler in the matrix causing enhancement in dynamic properties such as storage modulus

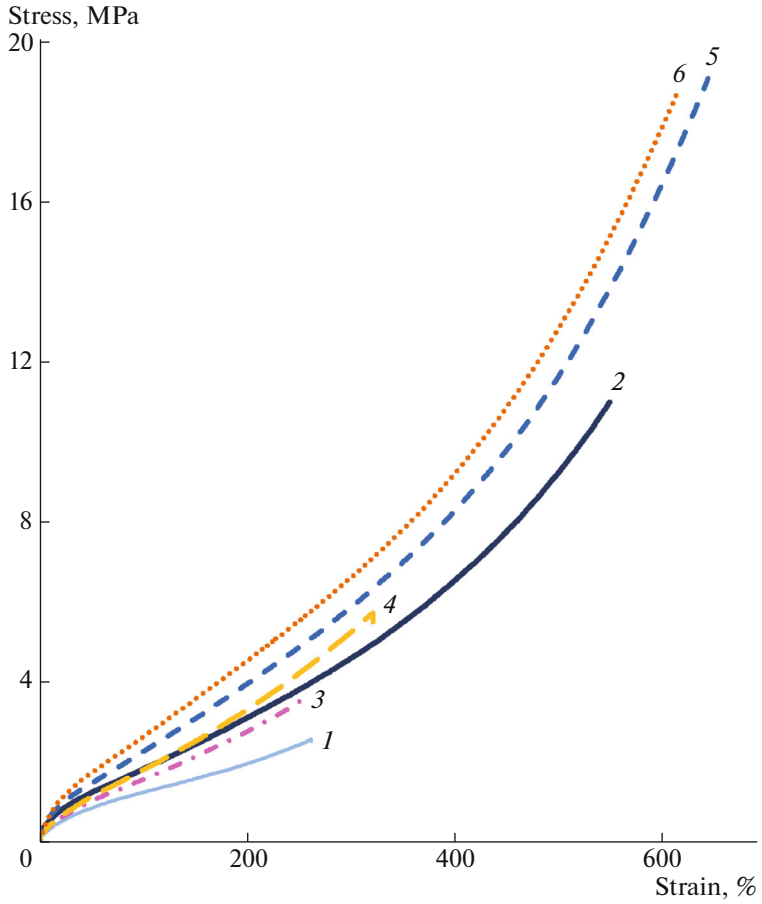

Fig. 7. (Color online) Typical tensile stress/strain curves of the NBR compounds: (*1*) NBR0:0, (*2*) NBR25:0, (*3*) NBR0:3, (*4*) NBR0:5, (*5*) NBR25:3, and (*6*) NBR25:5.

[19]. The same results were observed for nanoclay/carbon black and nanoclay/whiskers hybrid systems [4, 13].

To interpret the variation of the storage modulus of polymeric composites and to predict the reinforcing effect of colloidal fillers on elastomers, the values of elastic modulus are fitted to the several model that are exist in this respect. In this regard, Guth and Gold [20] introduced a quadratic term on the basis of the Smallwood-Einstein equation to take account of the interaction between filler particles, and obtained the following equation:

$$E = E_m[1 + 2.5\varphi + 14.1\varphi^2], \quad (2)$$

where E is Young's modulus of filled elastomer, E_m is matrix Young's modulus, and φ is the volume fraction of filler. Eq. (2) is only applicable to elastomers filled with a certain amount of spherical fillers. If the filler concentration is higher, the modulus increases much more rapidly than the Eq. (2) would predict. The reason can be attributed to the formation of a network involving spherical filler chains. Considering the chains composed of spherical fillers are similar to rod-like filler particles embedded in a continuous matrix, Guth later developed the following equation by introducing a shape factor, α, in order to account for this 'accelerated stiffening' [21].

$$E = E_m[1 + 0.67\alpha\varphi + 1.62(\alpha\varphi)^2], \quad (3)$$

where α is a filler shape factor defined as the ratio between the main and secondary axis of the filler particles. For reinforcing silica particles $\alpha \approx 7$ [23], and for CNT $\alpha \approx 25$ [23]. The volume fraction is expressed as:

$$\varphi = \{[\mathrm{phr}_{\mathrm{filler}}/\rho_{\mathrm{filler}}]/([\mathrm{phr}_{\mathrm{filler}}/\rho_{\mathrm{filler}}] + [\mathrm{phr}_{\mathrm{matrix}}/\rho_{\mathrm{matrix}}])\}, \quad (4)$$

where phr_x and ρ_x are the filler (matrix) phr and density, respectively.

The Guth Gold and Modified Guth Gold equations were employed to predict the modulus of NBR composites. Figure 6 shows the comparison of the model predictions with that of experimental values.

It can be observed that, value obtained by applying the original Guth Gold equation showed the higher deviations from the value obtained for another model

Table 4. Mechanical properties of the NBR compounds

Properties	NBR0:0	NBR25:0	NBR0:3	NBR0:5	NBR25:3	NBR25:5
Hardness, Shore A	50	58	52	53	60	64
Stress at 100% elongation, MPa	1.2	1.8	1.5	1.8	2.2	2.6
Stress at 200% elongation, MPa	1.9	3.1	2.7	3.2	3.9	4.5
Stress at 300% elongation, MPa	–	4.5	–	5.2	5.8	6.5
Tensile strength, MPa	2.5	11.1	3.6	5.7	19.0	18.7
Elongation at break, %	263.2	550.1	259.2	322.3	644.1	615.5
Burst strength, bar (g)	3.2	6.7	4.6	5.9	9.8	10.1

and the experimental values. This can be possible since the aspect ratio of the silica and/or CNT were not considered in the original Guth Gold equation.

However, the values derived from the modified Guth Gold equation show low deviation from the experimental results. It is worthy to note that the predicted values using this equation have been deviated considerably from the experimental values in case of samples containing hybrid reinforcing fillers. The values derived from the model matches well with that of experimental values for the silica filled NBR (NBR25:0) and CNT filled NBR (NBR0:3 and NBR0:5). This shows that the modified Guth Gold equation can take into consideration regarding the contribution of CNT and/or silica particles.

For hybrid samples (NBR25:3 and NBR25:5), the experimental values show a significant positive deviation from model predictions. This can be explained on the basis silica-CNT dual structure formation between silica particles and CNT tubes in hybrid samples. Moreover, it can be noticed that the immobilized polymer chains attached to the filler, can lead to an increase in effective volume fraction of the filler in the matrix causing enhancement in dynamic properties such as storage modulus. The Modified Guth Gold model does not take into account the aspect ratio of this structure formed by silica and CNT. Therefore, it can be stated that the dual structure and immobilized polymer chains are responsible for the synergistic effect observed in the mechanical and dynamic mechanical properties of hybrid samples.

Tensile properties. Figure 7 depicts stress-strain behavior for the NBR compounds containing different amounts of silica and CNTs. As expected, the tensile properties of compounds increases with the addition of reinforcing fillers, either CNT or silica. Table 4 summarizes the ultimate properties of tensile strength, elongation at break, stress at 100, 200 and 300% elongation, and hardness. The mechanical properties of the NBR compounds, such as the tensile strength, elongation at break, stress at different elongation and hardness relative to the pure NBR are enhanced because of the presence of reinforcing fillers.

The tensile strength and stress at 200% elongation for the 25 phr silica filled NBR vulcanizate (NBR25:0) were greater than that for the neat NBR vulcanizate, as expected because of the reinforcement effect and rigidity of silica in the NBR [11]. Loading the silica filler resulted in a progressive improvement of the tensile strength of the NBR25:0, the results being in line with the maximum torque results shown in Fig. 3.

Sample containing 5 phr CNT in NBR matrix (NBR0:5) shows a tensile strength of 5.7 MPa and elongation at break of 320%, respectively. It is interesting to note that CNT addition has resulted in a steady increase in percent elongation at break and this trend is in-line with the results published in literature for the other CNT based rubber-nanocomposites [6, 9]. However, it can be seen from Fig. 7 and Table 4 that sample containing 25 phr silica (NBR25:0) exhibits the higher tensile strength and elongation at break compared to those of CNT filled NBR (NBR0:3 and NBR0:5). The high amount and large surface areas of silica offer a strong reinforcement.

However, stress at 200 and 300% elongation is higher for NBR sample containing 5 phr CNT (3.3 and 5.2 MPa, respectively) compared to NBR sample containing 25 phr silica (3.1 and 4.6 MPa, respectively. The higher modulus value for CNT filled compounds may be attributed to the network structure of CNT [9], which leads to the occlusion of rubber chains within the CNT structure.

Surprisingly, NBR samples containing combination of silica and CNT (NBR25:3 and NBR25:5) show an increase in strength properties of the composites. Addition of 3 phr CNT to the NBR sample containing 25 phr silica shows an increased tensile strength value of 19 MPa. This value is exactly 71% compared to the tensile strength value of the NBR25:0. This suggests a synergistic effect between the silica and CNT. Moreover, at high strains, stress-hardening behavior is observed for these hybrid samples. The tube arrangement of CNT allows for chain slippage thus preventing the breakage of molecules at higher strains while the bound rubber in silica structure contributes to the modulus and strength. It is important to mention here

that the elongations at break for the hybrid systems are remarkably higher than that of silica or CNT filled compounds. This can be explained by considering the partial break down of network structure of silica in NBR hybrid nanocomposites (NBR25:3 and NBR25:5). These results are in agreement with the DMTA results.

Burst strength. Many industries, such as petrochemical, chemical, pharmaceutical, food processing, and oilfield applications, rely on pressurized equipment and assemblies such as pressure vessels and propellant subsystems. Burst diaphragms, also referred to as bursting discs and rupture discs, as pressure relief devices, sacrificially protect mission-critical systems from predetermined differential pressure, either positive or negative, that is, over pressurization and potentially damaging vacuum conditions. Major advantages of the use of rupture discs compared to pressure relief valves would be leak tightness, no maintenance and cost. Burst discs usually have steel or aluminum housings enveloping a one-time-use membrane commonly made of cold-rolled steel, nickel alloys, aluminum, or any other material with yield strength close to its ultimate strength. Nitrile rubber and hydrogenated Nitrile Butadiene Rubber, as a family of unsaturated copolymers of acrylonitrile (ACN), are commonly used to produce such diaphragms operating up to 120°C. NBR is resistant to aliphatic hydrocarbons, oil, and fuel and hence is selected for this study contemplated for oilfield applications.

There is a mathematical formula that calculates the relationship of internal pressure to allowable stress, nominal thickness, and diameter of the sphere. Simply stated, Barlow's formula calculates the pressure containing capabilities of a component [3]. The formula takes into account the sphere diameter (D), diaphragm thickness (t), and the manufacturer's specified minimum yield strength of the component (S):

$$P = 4St/D. \quad (5)$$

In elastomers, the component effective thickness depends on the material elongation capability. To modify the formula for the present application, λ is entered as the elongation at break. Finally, we will have

$$P = 400St/D\lambda. \quad (6)$$

According to Eq. (6), the ratio of tensile strength to elongation at break plays a key role in burst strength. As it can be seen in Table 4, hybrid compounds (NBR25:3 and NBR25:5) show higher burst strength compared to silica or CNT filled NBR compounds. It may be attributed to the synergistic effect between the silica and CNT in NBR matrix.

CONCLUSIONS

The effects of silica, carbon nanotubes and silica/carbon nanotubes hybrid filler on mechanical and vulcanization characteristics of the NBR compounds were investigated. The results of SEM show that the both reinforcing fillers have good dispersion and distribution in NBR matrix. The optimum cure time and scorch time both decrease with adding the silica to NBR compounds. This phenomenon can be explained by increasing in the compound viscosity and thus the shear heating effect in the silica filled NBR compounds. Also, it may be due to the increase in effective filler volume by bound rubber for the silica. Considerable improvements in dynamic storage modulus and a steady decrease in tan δ (highest) values are observed in case of NBR compounds with use of silica/CNT hybrid fillers. This can be the consequence of good polymer-filler interaction. The theoretical modelling of NBR compounds has been done using the Guth Gold and the modified Guth Gold equations. The models' predictions fit well with the experimental values for the silica and CNT filled NBR compounds. The experimental values have shown a positive deviation for hybrid systems. This can be explained on the basis silica-CNT dual structure formation between silica particles and CNT tubes in hybrid samples. Moreover, NBR samples containing combination of silica and CNT show an increase in strength properties of the composites. Addition of 3 phr CNT to the NBR sample containing 25 phr silica shows an increased tensile strength value of 19 MPa. This value is exactly 71% compared to the tensile strength value of the silica filled NBR. This suggests a synergistic effect between the silica and CNT. According to this synergistic effect the hybrid compounds show higher burst strength compared to simple compounds, this is confirmed by the suggested formula according to Barlow's equation.

REFERENCES

1. S. Chen, H. Yu, W. Ren, and Y. Zhang, Thermochim. Acta **491**, 103 (2009).
2. D. Chayan and K. Bharat, Res. J. Recent Sci. **1**, 357 (2012).
3. A. A. Davoodi, T. Khalkhali, M. M. Salehi, and S. Sarioletlagh Fard, J. Soft Matter **2014**, 498563 (2014).
4. S. Praveen, P. K. Chattopadhyay, P. Albert, V. G. Dalvi, B. C. Chakraborty, and S. Chattopadhyay, Composites, Part A **40**, 309 (2009).
5. H. Ismail and H. S. Ahmad, Polym.–Plast. Technol. Eng. **52**, 1175 (2013).
6. L. D. Perez, M. A. Zuluaga, T. Kyu, J. E. Mark, and B. L. Lopez, Polym. Eng. Sci. **49**, 866 (2009).
7. W. G. Hwang, K. H. Wei, and C. M. Wu, Polym. Eng. Sci. **44**, 2117 (2004).
8. Q. Li, S. Zhao, and Y. Pan, J. Appl. Polym. Sci. **117**, 421 (2010).
9. B. Likozar and Z. Major, Appl. Surf. Sci. **257**, 656 (2010).

10. S. Ostad Movahed, A. Ansarifar, and F. Mirzaie, J. Appl. Polym. Sci. **132**, 41512 (2015).
11. N. Sombatsompop, E. Wimolmala, and C. Sirisinha, J. Appl. Polym. Sci. **110**, 2877 (2008).
12. S.M. Hosseini and M. Razzaghi-Kashani, Polymer **55**, 6426 (2014).
13. A. Bendahou, H. Kaddami, E. Espuche, F. Gouanvé, and A. Dufresne, Macromol. Mater. Eng. **296**, 760 (2011).
14. F. Y. Yuan, H. B. Zhang, X. Li, X. Z. Li, and Z. Yu, Composites, Part A **53**, 137 (2013).
15. H. Yan, K. Sun, Y. Zhang, and Y. Zhang, Polym. Test. **24**, 32 (2005).
16. J. Lee, J. Hong, D. W. Park, and S. E. Shim, Macromol. Res. **17**, 718 (2009).
17. M. J. Wang, S. Wolff, and J. B. Donnet, Rubber Chem. Technol. **64**, 559 (1991).
18. S. S. Choi, B. H. Park, and H. Song, Polym. Adv. Technol. **15**, 122 (2004).
19. N. Rattanasom, T. Saowapark, and C. Deeprasertkul, Polym. Test. **26**, 369 (2007).
20. E. Guth and O. Gold, Phys. Rev. **53**, 322 (1938).
21. Y. P. Wu, O. X. Jia, D. S. Yu, and L. Q. Zhang, Polym. Test. **23**, 903 (2004).
22. N. Z. Noriman and H. Ismail, Int. J. Polym. Mater. Polym. Biomater. **62**, 252 (2013).
23. F. Cataldo, O. Ursini, and G. Angelini, Fullerenes, Nanotubes, Carbon Nanostruct., No. 17, 38 (2009).